The ROYAL COLLEGE of
OPHTHALMOLOGISTS

ARTICLE

Quantitative OCT angiography findings according to pattern classification of type 1 neovascularization exudative age-related macular degeneration

Mihyun Choi[1] · Somin Ahn[1] · Cheolmin Yun[2] · Seong-Woo Kim [1]

Abstract

Objectives To define neovascularization (NV) patterns and their association with exudative activity in type 1 neovascular age-related macular degeneration (NVAMD).

Methods In optical coherence tomography angiography (OCTA) images of type 1 NVAMD, we stratified NV patterns according to whether they contained core vessel (C+/C−) and fine branching vessels (F+/F−) or not into C − F +, C + F +, and C + F − groups. Qualitative analyses assessing the status of peripheral tiny branching, inner branching capillaries, arcade, loop, and perilesional halo and quantitative analyses considering the NV area, length, density, and numbers of junctions and endpoints (open-ended vessels) in NV were conducted according to NV patterns and the presence of exudation on structural OCT.

Results Among 96 eyes, exudation was found in the C − F + (33.3%) and C + F + (47.6%) groups, related to peripheral tiny branching in both groups ($p = 0.022$ and $p < 0.001$) and perilesional halo in the C + F + group ($p < 0.001$). Peripheral arcades, inner branching capillaries, and loops were observed in more than half (68.3%, 58.7%, and 69.8%) in the C + F + group but not related with exudative activity in the C + F + group. In quantitative analysis, the number of endpoints was associated with exudation in univariate and multivariate analyses ($p = 0.011$ and $p = 0.016$) in C + F + group.

Conclusions After pattern classification, type 1 NV patterns with fine branching vessels were considered to have exudative activity compared to NV without fine branching. The quantitative analysis of type 1 NV according to patterns showed the presence of peripheral tiny branching vessels was associated with NV activity.

Introduction

Neovascular age-related macular degeneration (AMD) is a vision-threatening disease associated with angiogenesis of neovascularization (NV) [1]. The progression of OCT angiography (OCTA) technology has allowed for non-invasive and depth-resolved visualisation of the chorioretinal vasculature [2, 3], and improved research, diagnosis, and surveillance in the AMD population [4]. From early OCTA studies onward, many researchers have analysed the characteristics of NV and suggested patterns for NV, such as "sea fan," "medusa," or "dead tree," according to vascular morphology [5, 6]. Most pattern classifications are focused on the presence of a trunk vessel in the NV lesion [7–9], which was thought to be pericyte-covered, resistant to anti-VEGF therapy. However, the classification scheme varies among researchers and tends to be subjective in nature.

When identifying qualitative biomarkers of disease activity in AMD, researchers observed the significance of the detailed lesion components of the NV. The presence of tiny branching vessels, peripheral arcades, a perilesional halo [10] and peripheral higher fractal dimension [11] were proposed as active (exudative) biomarkers. However, identification of these qualitative biomarkers necessitates subjective judgments, and the question remains whether

these active biomarkers could be applicable to each NV pattern. To understand the disease in depth using OCTA and to develop further treatment strategies, it is very important to analyse both the NV pattern and the detailed lesion components together as biomarkers of disease activity in AMD. Nevertheless, quantitative studies concerning NV morphologic patterns and their detailed components have been lacking until now.

The primary purpose of this study was to quantify patterns of NV according to the conventional classification scheme based on OCTA. Secondarily, each pattern of NV was characterised and compared with regard to the activity of the exudative AMD, considering the detailed lesion components and the quantitative index.

Subjects and methods

This was a retrospective, cross-sectional review of medical records of 112 patients with NVAMD at the Korea University Guro Hospital between February 2018 and February 2020. The Institutional Review Board (IRB) of Korea University Medical Center approved this study (IRB no. 2019GR0217) and all research and data collection processes were conducted in accordance with the tenets of the Declaration of Helsinki.

Patient selection

Patients had to meet the following criteria to be eligible for inclusion: (1) diagnosis of subfoveal type 1 NVAMD by multimodal imaging (fluorescein angiography, indocyanine green angiography, and structural OCT); (2) age >50 years; (3) received a previous loading dose of 3 monthly intravitreal injections (IVI); (4) had a treatment protocol only involved aflibercept (Eylea; Regeneron Pharmaceuticals, Tarrytown, NY, USA) with "pro-re-nata" regimen based on structural OCT findings [12]; (5) had received aflibercept injection within the last 2 months and a minimum interval of 1 month between the last IVI and the OCTA examination; and (6) a best-corrected visual acuity (BCVA) of better than 20/100. Exclusion criteria for the study included types 2 and 3 NV or polypoidal choroidal vasculopathy, a history of central serous chorioretinopathy, large pigment epithelial detachment (PED), NV fibrotic scarring, atrophic changes at the fovea, or any concurrent vascular obstructive retinal disease. Patients previously treated with photodynamic therapy and treated at other institutions were excluded from the analysis. BCVA, slit-lamp examination, and dilated funduscopic examination were performed, and spectral-domain OCT and OCTA images were obtained at the analysis point. We defined exudation with spectral-domain OCT including the presence of intraretinal fluid and subretinal fluid. An IVI was given in the case of evidence of exudation on OCT and patients were followed up based on the "pro-re-nata" protocol. For patients who were followed up for more than 12 months from the time of OCTA analysis, the presence or absence of exudation recurrence, the number of IVIs for 12 months, and the period of recurrence (months) were additionally investigated.

Image acquisition

Structural OCT and OCTA images were obtained using a spectral-domain OCT device (Spectralis OCT2; Heidelberg Engineering, Heidelberg, Germany). The OCTA scan covered a 4.3×4.3 mm ($15° \times 15°$) area centred on the fovea. CRT measurements were obtained on a thickness map (circle diameter of 1 mm) and SFCT measurements were manually measured as described in previous studies [13, 14]. The slab containing type 1 NV was defined using fusion images of structural OCT and OCTA from the external limiting membrane to the line of Bruch's membrane using the software HEYEX (Heidelberg Engineering, Heidelberg, Germany) (Fig. 1) [15]. A retinal specialist (M. C.) confirmed the location of the auto-segmented line, making manual adjustments as needed. NV images were processed using the open-source GNU Image Manipulation Program (GIMP) version 2.8.14 to manually eliminate projection artifacts and subthreshold signals (Fig. 2).

Image analysis

All images were evaluated by two independent graders (M. C. and S. M. A.) after assigned unique numbers, with discrepancies in grading resolved through adjudication by a senior image grader (S. W. K.). The presence of exudation was determined on structural OCT and the patterns of the neovascular membranes on OCTA were evaluated and categorised based on the following according to a modified version of the method of Xu et al. [7] (1) whether the lesion contains a large core (trunk) vessel (presence: C+, absence: C−) and (2) whether the lesion has fine branching vessels (presence: F+, absence: F−) into C − F+, C + F+, and C + F − groups. The core vessel diameter similar to or greater than arteriole in an en-face retinal vasculature slab (from ILM to BM) was defined as core vessel–positive (C+) (Fig. 1). This was based on previous reports suggesting the calibre of the core vessel in type I NV is 39.52–98.52 μm [15, 16] and that of the retinal arteriole is 32.4–112.2 μm (depending on the measurement location) using OCTA [17, 18]. The NVs showing a C + F + pattern was further divided into two subgroups, symmetrical and asymmetrical growth (previously referred to as a medusa pattern and sea-fan pattern) (Fig. 1B, C). NVs where none
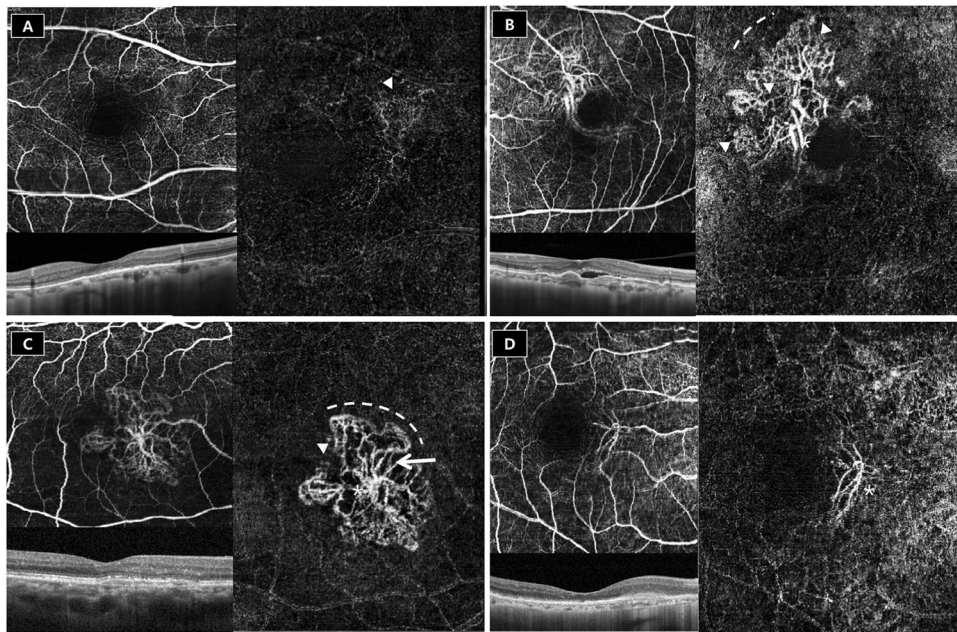
Fig. 1 The morphologic patterns of NV (type 1) of neovascular AMD in this study. (Left top) retinal slab of an en-face OCT image (ILM to BM), (Left bottom) cross-sectional OCT, (Right) NV slab of the en-face OCTA. **A** The NV slab shows the "C − F + group" of type 1 NV with peripheral tiny branching capillaries (white arrowhead). In the retinal slab, the core vessel of NV cannot be found. The cross-sectional OCT shows no fluid accumulation. **B** The "C + F + group" of type 1 NV with asymmetrical growth containing dilated core vessels (*) presented as larger than the arteriole diameter in the retinal slab. NV also has branching capillaries in the lesion interior (yellow arrowhead), perilesional halo in the superior part (white dashed line), and peripheral tangled branching capillaries (white arrowhead). The cross-sectional OCT shows subretinal fluid accumulation. **C** The "C + F + group" of type 1 NV with symmetrical growth containing dilated central core vessels (*) with branching capillaries in the lesion interior (yellow arrowhead), internal loop (white arrow), and peripheral arcade (yellow dashed line). No fluid exudation found in cross-sectional OCT. **D** The "C + F − " group with finger-like growth NV containing dilated central core vessels (*) but no fine branching vessels and exudation.
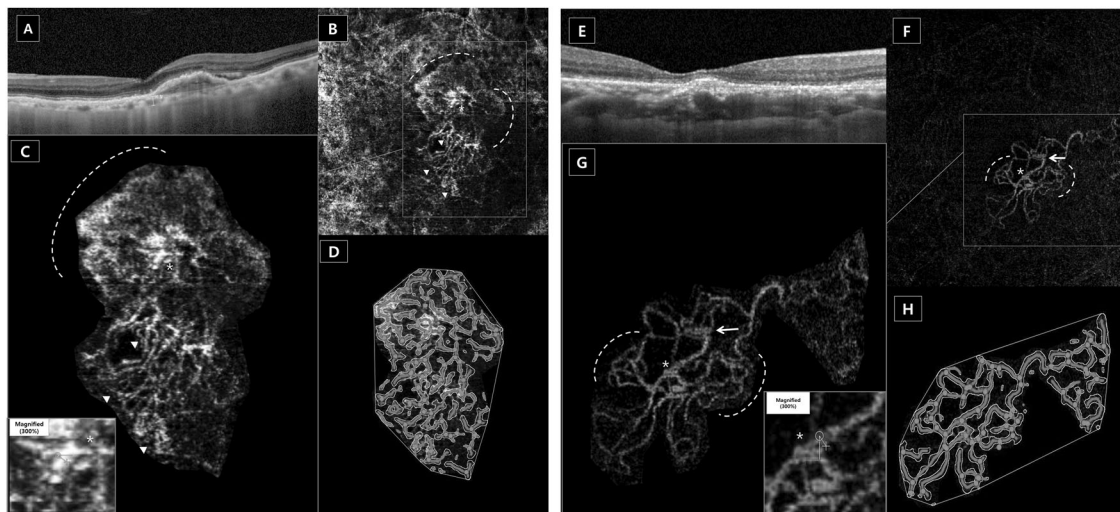
Fig. 2 Structural OCT and OCTA analysis in this study. Structural OCT and OCTA analysis in patients (**A–D**) with focal exudation in the subretinal space, (**E–G**) without exudation in structural OCT. **A**, **E** Structural OCT (vertical image at fovea). **B** The NV slab in the en-face OCTA image shows the "symmetrical growth pattern" of C + F + group NV containing dilated core vessels (*), peripheral arcade (yellow dashed line), perilesional halo (white dashed line) and peripheral tangled branching capillaries (white arrowhead). **F** The NV slab shows the "asymmetrical growth pattern" of C + F + NV containing dilated core vessels (*), peripheral arcade (yellow dashed line) and internal loop (white arrow). **C**, **G** Manually cropped image of NV to remove projection artifacts (inlet: NV image magnified by 300%; pixels between O and X were calculated to measure the vessel calibre). **D**, **H** AngioTool analysis, skeletonized vessel (red line), junction point (blue dot), vessel area (outer green line), and endpoint (point of the open-ended vessel).

of the above characteristics (ill-defined) fit were excluded from the analysis.

For detailed lesion components, the following five OCTA qualitative features were adopted as biomarkers of NV activity as initially described by Coscas et al. [10, 19] but modified for the current study: (1) presence of tiny branching vessels (i.e. thin, fringed, tangled capillaries) in the periphery of the lesion; (2) presence of interior (in NV) branching capillaries; (3) presence of a peripheral anastomotic arcade; (4) presence of inner loops; and (5) presence of a perilesional hypointense halo (Figs. 1, 2). The largest vessel calibre measured with 300% magnified image in GIMP (Fig. 2C, G).

For quantitative analysis, AngioTool (version 0.6a; National Cancer Institute, Center for Cancer Research, Bethesda, MD, USA) which provides following parameters was applied to OCTA NV images (Fig. 2D, H) [9, 20, 21]: (1) vessel area, (2) vessel density (i.e. ratio of the area occupied by vessels in the NV lesion), (3) total number of junctions (i.e. number of junctions in segmented vessels), (4) total number of endpoints (i.e. number of open-ended segments), (5) total length of vessel (i.e. sum of Euclidean distances between the pixels of all the vessels in the image), and (6) mean lacunarity (i.e. mean lacunarity among all-sized boxes) [21]. The junction density (i.e. total number of junctions/total length of vessel) and endpoint density (i.e. total number of endpoint/total length of vessel), both in n/mm, were calculated in the same manner as that adopted in previous studies [15, 22].

Statistical analysis

All statistical procedures were performed using the Statistical Package for the Social Sciences version 22 (IBM Corp., Armonk, NY, USA). For qualitative (subjective) variables, intergrader kappa coefficients were accessed by using the chi-squared test. The presence of qualitative active biomarkers and quantitative values of NV were compared between three morphologically classified groups (C − F + , C + F + , C − F −) using the chi-squared test for categorical variables or one-way analysis of variance (ANOVA) test or Kruskal–Wallis test for continuous variables; if the results were significant, post-hoc analysis was added. To consider multiplicity in statistical comparisons, the Bonferroni correction was applied during post-hoc analysis and the outcome was considered significant when $p < 0.017$ (0.05/3). Correlations between OCTA quantitative values were verified using Pearson's correlation coefficient (CC) including all three groups together. The univariate and multivariate binary logistic regression (exudation vs. non-exudation) for quantitative values were also evaluated.

Results

A total of 112 patients met the patient selection criteria; however, 16 were subsequently excluded either due to poor image quality or ungradable (ill-defined) OCTA images. Thus, a total of 96 patients ($n = 58$ males) were finally included in the study, with a mean age of 75.66 ± 6.16 (range: 57–90) years. Based on NV pattern, there were 18 eyes (18.8%) included in the C − F + group, 63 eyes (65.6%) included in the C + F + group, and 15 eyes (15.6%) included in the C + F − group. The kappa value for the pattern classification between the two testers was 0.753, which suggested moderate agreement. The baseline demographics of the three groups are summarised in Table 1. There were no significant differences in terms of age, sex,

Table 1 Patient demographics.

	C − F + (n = 18)	C + F + (n = 63)	C + F − (n = 15)	P value
Mean age (SD)	75.66 (6.16)	73.13 (6.73)	73.75 (6.89)	0.369
Sex (M/F)	8/10	39/24	11/4	0.220
Time from diagnosis (months), mean (SD)	22.64 (19.74)	18.72 (16.95)	13.78 (11.09)	0.113
Previous anti-VEGF treatments, mean (SD)	6.28 (5.08)	6.72 (4.49)	3.56 (2.19)	**0.037***
LogMAR BCVA, mean (SD)	0.31 (0.24)	0.35 (0.24)	0.39 (0.35)	0.285
CRT (μm), mean (SD)	253.73 (43.95)	264.56 (83.00)	233.75 (27.29)	0.124
SFCT (μm), mean (SD)	208.13 (67.27)	196.14 (80.34)	174.68 (59.64)	0.393

C − F + = NV lesions without core vessels but containing fine branching vessels.

C + F + = NV lesions with lesion with large core vessel and fine branching vessels.

C + F − = NV lesions with lesion with large core vessel without branching capillaries.

SD standard deviation, *VEGF* vascular endothelial growth factor, *BCVA* best-corrected visual acuity, *CRT* central retinal thickness, *SFCT* subfoveal choroidal thickness.

*Post-hoc analysis: *p* value for C − F + vs. C + F − = 0.050, **C + F + vs. C + F − = 0.01**, C − F + vs. C + F + = 0.743.

mean time from diagnosis, or BCVA. The number of previous IVI treatments revealed a significant difference between the three groups (6.28 vs. 6.72 vs. 3.56, $p = 0.037$), and post-hoc analysis indicated that this difference was caused by a variation between the $C + F +$ and $C + F -$ groups ($p = 0.01$). There were no differences in CRT or SFCT among the three NV pattern classifications (Table 1).

Qualitative and quantitative OCTA features according to NV patterns

Six eyes in the $C - F +$ group (33.3%) and 30 eyes in the $C + F +$ group (47.6%) showed exudation on structural OCT ($p = 0.282$), while all of the $C + F -$ group showed no exudation ($p = 0.003$). In OCTA image qualitative (subjective) analysis, the intergrader kappa coefficient was 0.676 ($p < 0.001$), indicating substantial agreement. When comparing the presence of qualitative OCTA biomarkers in three groups (Table 2), the presence of peripheral tiny branching was higher in the $C - F +$ (27.8%) and $C + F +$ (54.0%) groups than in the $C + F -$ group (0%) (p values for $C - F +$ vs. $C + F - = 0.013$ and $C + F +$ vs. $C + F - < 0.001$). However, there was no difference between the $C - F +$ and $C + F +$ groups ($p = 0.063$). Inner branching capillaries, peripheral arcade, and loop were most frequently observed in the $C + F +$ group (58.7%, 68.3%, and 69.8%; all $p \leq 0.001$). During quantitative analysis (Table 2), the $C + F +$ group showed the most remarkable difference relative to the other two groups, with the largest NV area (1.53 ± 0.92 mm^2) and the longest total NV length (24.72 ± 15.07 mm) (all $p < 0.001$). The NV density of the $C + F +$ group was lower than that of the $C + F -$ group ($p = 0.005$). While the junction and endpoint numbers were highest in the $C + F +$ group (82.48 ± 55.36 and 81.98 ± 48.96) (all $p < 0.001$), there was no significant difference among the three groups in terms of junction or endpoint density. The core vessel calibre (µm) was larger in the $C + F +$ group than in the $C + F -$ group (58.91 ± 16.57 vs. 47.69 ± 19.28, $p = 0.017$). For Pearson's CC coefficient analysis considering all three groups together, the total vessel length was strongly correlated with the vessel area (CC = 0.997; $p < 0.001$), junction number (CC = 0.981; $p < 0.001$), and endpoint number (CC = 0.913; $p < 0.001$) but negatively correlated with NV density (CC = −0.289; $p = 0.004$).

Comparative analysis of OCTA according to exudation

Since no exudation was observed in the $C + F -$ group, the qualitative and quantitative features between active (exudative) and inactive (non-exudative) lesions was compared only in the $C - F +$ and $C + F +$ groups (Table 3).

Peripheral tiny branching was significantly associated with active lesions in both the $C - F +$ [$p = 0.022$, odds ratio (OR): 22.0 (95% confidence interval (CI): 1.54–314.29)] and $C + F +$ [$p < 0.001$; OR: 20.31 (95% CI: 5.42–76.02)] groups. Inner capillary branching, peripheral arcade, and loops were not significantly different depending on activity. In the $C + F +$ group, perilesional halo was more frequently observed in eyes with exudation [$p < 0.001$; OR: 13.56 (95% CI: 2.74–67.16)].

The quantitative values between the active and inactive lesions showed significant differences only in the $C + F +$ group. In the $C + F +$ group, active lesions had a larger NV area (1.81 ± 0.79 mm^2 vs. 1.29 ± 0.95 mm^2; $p = 0.022$) and longer total NV length (29.22 ± 12.95 mm vs. 20.81 ± 15.74 mm; $p = 0.025$) than inactive lesions. Also, the numbers of junctions (98.83 ± 47.72 vs. 68.03 ± 57.61; $p = 0.025$) and endpoints (99.40 ± 46.09 vs. 66.42 ± 45.97; $p = 0.006$) were significantly higher in active lesions. Findings from univariate and multivariate binary logistic regression analyses involving quantitative OCTA variables associated with the exudative state in the $C + F +$ group are Supplementary Table S1. In univariate binary logistic regression analyses, NV area, length and the number of endpoints and junction were significantly related with exudation ($p = 0.028$, 0.031, 0.011 and 0.034, respectively). But in a multivariate analysis, only endpoint number was associated with exudation [Exp(B) = 1.055 [95% CI: 1.004–1.084]; $p = 0.016$] ($p = 0.305$ in NV area, 0.108 in NV length and 0.059 in the number of junctions).

In additional qualitative and quantitative analyses of OCTA according to growth pattern (symmetric vs. asymmetric) in the $C + F +$ group (Supplementary Table S2), there were no differences in the presence of exudation on structural OCT or active biomarkers between the two groups. During quantitative analysis, the asymmetrical growth group showed a higher degree of lacunarity, suggesting the lesion was more inhomogeneous relative to the symmetrical growth group (0.228 vs. 0.280; $p = 0.033$), while no other difference was found between the two growth patterns in the $C + F +$ group.

Follow up analysis

In patients who were followed up for more than 12 months from the time of OCTA analysis ($n = 88$), the average numbers of IVIs during 12 months were 1.82 ± 1.59 in the $C - F +$ group, 2.98 ± 1.53 in the $C + F +$ group, and 1.86 ± 1.30 in the $C + F -$ group. The number of IVIs was significantly higher in $C + F +$ group ($p = 0.004$, post-hoc analysis, $C - F +$ vs. $C + F + = 0.018$, $C + F +$ vs. $C + F - = 0.034$). In patients who were followed up for 12 months, 55 eyes showed no exudation at the time of OCTA analysis ($C - F + = 12$, $C + F + = 28$, $C + F - = 15$).

Table 2 Qualitative and quantitative OCTA features according to NV patterns.

	C − F+ (n = 18)	C + F+ (n = 63)	C + F− (n = 15)	P value Comparing 3 groups[a]	C − F+ vs. C + F+	C − F+ vs. C + F−	C + F+ vs. C + F−
Exudation, n (%)	6 (33.3)	30 (47.6)	0	**0.003**	0.282	**0.011**	**<0.001**
Morphological feature, n (%)							
Peripheral tiny branching	5 (27.8)	34 (54.0)	0	**0.001**	0.063	**0.013**	**<0.001**
Inner branching capillaries	3 (16.7)	37 (58.7)	2 (13.3)	**<0.001**	**0.003**	1.000	**0.003**
Arcade	3 (16.7)	43 (68.3)	1 (6.7)	**<0.001**	**<0.001**	0.607	**<0.001**
Loops	0	44 (69.8)	5 (33.3)	**<0.001**	**<0.001**	**0.013**	**0.016**
Halo	2 (11.1)	16 (25.4)	0	**0.050**	0.335	0.489	0.032

Quantitative features, mean (SD)	C − F+ (n = 18)	C + F+ (n = 63)	C + F− (n = 15)	Comparing 3 groups[b]	C − F+ vs. C + F+	C − F+ vs. C + F−	C + F+ vs. C + F−
NV area (mm^2)	0.63 (0.34)	1.53 (0.92)	0.66 (0.49)	**<0.001**	**<0.001**	0.979	**<0.001**
NV density (mm/mm^2)	0.44 (0.06)	0.41 (0.06)	0.47 (0.09)	**0.014**	0.169	0.437	**0.005**
Total NV length (mm)	10.54 (7.03)	24.72 (15.07)	10.42 (8.22)	**<0.001**	**<0.001**	0.941	**<0.001**
Junction number	36.22 (22.27)	82.48 (55.36)	30.87 (25.55)	**<0.001**	**0.001**	0.822	**<0.001**
Endpoint number	41.66 (27.68)	81.98 (48.96)	33.00 (28.12)	**<0.001**	**0.002**	0.676	**<0.001**
Junction density (n/mm)	55.65 (17.25)	52.55 (8.10)	46.38 (11.28)	**0.044**	0.526	0.038	0.112
Endpoint density (n/mm)	63.18 (24.53)	54.13 (15.19)	47.21 (3.76)	**0.028**	0.122	0.026	0.363
Lacunarity	0.237 (0.093)	0.258 (0.113)	0.262 (0.116)	0.745			
Core vessel caliber (μm)		58.91 (16.57)	47.69 (19.28)				**0.017**

C − F+ = NV lesions without core vessels but containing fine branching vessels.

C + F+ = NV lesions with lesion with large core vessel and fine branching vessels.

C + F− = NV lesions with lesion with large core vessel without branching capillaries.

Considered significantly when $p < 0.05$ in comparing three group and $p < 0.017$ in post-hoc analysis. Significant p values are presented in bold.

NV Neovascularization.

[a]Chi-squared test was applied; when the number of variables was <5, the Fisher's exact test was applied.

[b]One-way ANOVA. Post-hoc analysis with Tukey's method when the ANOVA test showed significant results.

Table 3 Comparison of qualitative and quantitative features of NV between exudative and nonexudative NV in C − F + and C + F + pattern NV.

Morphological feature, n (%)	C − F + group (18)			C + F + group (63)		
	Active	Inactive	p value[a]	Active	Inactive	p value[a]
	6 (33.3)	12 (66.7)		30 (47.6)	33 (52.4)	
Peripheral tiny branching	4 (66.7)	1 (8.3)	**0.022**[c]	26 (86.7)	8 (24.2)	**<0.001**[d]
Inner branching capillaries	1 (16.7)	2 (16.7)	1.000	19 (63.3)	18 (54.5)	0.479
Arcade	2 (33.3)	1 (8.3)	0.180	22 (73.3)	21 (63.6)	0.409
Loops	0	0	NA	21 (70)	23 (69.7)	0.979
Halo	1 (16.7)	1 (8.3)	1.000	14 (46.7)	2 (6.1)	**<0.001**[e]

Quantitative value, mean (SD)	C − F + group (18)			C + F + group (63)		
	Active	Inactive	p value[b]	Active	Inactive	p value[b]
	6 (33.3)	12 (66.7)		30 (47.6)	33 (52.4)	
NV area (mm^2)	0.54 (0.18)	0.67 (0.39)	0.473	1.81 (0.79)	1.29 (0.95)	**0.022**
NV density (mm/mm^2)	0.44 (0.04)	0.45 (0.06)	0.751	0.41 (0.06)	0.42 (0.07)	0.467
Total NV length (mm)	9.41 (4.84)	11.10 (6.48)	0.150	29.22 (12.95)	20.81 (15.74)	**0.025**
Junction number	31.66 (24.27)	38.50 (21.94)	0.556	98.83 (47.72)	68.03 (57.61)	**0.025**
Endpoint number	41.33 (33.94)	41.83 (25.70)	0.972	99.40 (46.09)	66.42 (45.97)	**0.006**
Junction density (n/mm)	54.16 (22.49)	56.39 (15.11)	0.804	53.88 (7.73)	51.24 (8.24)	0.196
Endpoint density (n/mm)	69.54 (22.49)	60.01 (20.46)	0.454	55.53 (13.02)	52.63 (16.85)	0.451
Lacunarity	0.250 (0.051)	0.231 (0.111)	0.697	0.254 (0.116)	0.265 (0.111)	0.688
Core vessel caliber (μm)				61.31 (17.34)	56.74 (15.80)	0.286

C − F + = NV lesions without core vessels but containing fine branching vessels.

C + F + = NV lesions with lesion with large core vessel and fine branching vessels.

NV Neovascularization, SD standard deviation.

[a]Fisher's exact test or Chi-squared test. Significant p values ($p < 0.05$) are presented in bold.

[b]T-test or Mann Whitney test. Significant p values ($p < 0.05$) are presented in bold.

Risk analysis with exudation on structural OCT

[c]Odds ratio 22.0 (1.54–314.29).

[d]Odds ratio 20.31 (5.42–76.02).

[e]Odds ratio 13.56 (2.74–67.16).

Of these 55 eyes, only 8 eyes (14.5%) did not show recurrence of exudation for 12 months. According to NV patterns, 4 eyes (33.3%) in the C−F + group ($n = 12$), 1 eye (3.6%) in the C + F + group ($n = 28$), and 3 eyes (20%) in the C + F− group ($n = 15$) showed no exudation on structural OCT for 12 months. In the C + F + group, the number of patients who did not show exudation for 12 months was significantly less than the other two groups ($p = 0.035$). The average months for exudation recurrence from last IVI was 6.75 ± 2.60 in the C−F + group, 5.88 ± 2.96 in the C + F + group, and 5.41 ± 3.80 in the C + F− group ($p = 0.651$).

Discussion

With the development of high-resolution OCTA, the morphological characteristics have been described by many researchers. Kuehlewein et al. identified NV as distinct (including the medusa and sea-fan patterns) and indistinct [6]. Sulzbacher et al. suggested a new classification scheme involving a dense-net configuration, loose-net configuration, and unidentifiable pattern [23]. Miere et al. categorised NV on OCTA as immature (including medusa, sea-fan, and indistinct) and mature (pruned vascular tree) patterns and suggested that mature NV is the result of remodelling induced by recurrent IVI treatment [8]. Xu et al. classified type 1 NV into three forms; immature, mature (lesion with large dilated vessels with branching capillaries), and hypermature (dead tree appearance) [7]. As seen in many studies, there were slight differences in terms of both NV classification and definition. Therefore, in this study, NV was more objectively categorised based on the presence of core vessels and branching capillaries in the lesion. In spite of the various classifications of NV reported in the past studies, researchers found that the C + F − pattern NV (also referred to as the dead tree, flinger-like, hypermature, or mature pattern) was consistent with lesion chronicity and inactivity [24, 25], whereas C − F + and C + F + patterns (medusa, sea-fan, immature), could be associated with either active or inactive disease [7, 23].

Previously, the presence of peripheral tiny branching vessels, arcade, loop, and perilesional halo were reported to

be associated with active NV [10, 11] and many researchers adopting these features as OCTA biomarkers reflecting exudation on structural OCT [9, 20]. In our study, the presence of peripheral tiny branching capillaries were correlated with active lesions in the C − F + and C + F + groups. But interestingly, peripheral arcades, inner branching capillaries, and loops were observed in more than half (68.3%, 58.7%, and 69.8%) in the C + F + group, revealing much higher prevalence rates than in the C − F + and C + F − groups, while no differences were found between active and inactive lesions in the C + F + group. Further, although 33.3% of the C − F + group (*n* = 6 eyes) had exudation on structural OCT, arcade and inner capillaries were found only in two eyes (33.3%) and one eye (16.7%), respectively, and loops were not found in any of the C − F + group at all, which were much lower than that in the exudative C + F + group. This result suggests that peripheral arcades, loops, and inner branching capillaries are characteristics of the type 1 NV pattern containing core vessel and fine branching (C + F +) rather than biomarkers of exudation. The repeated IVI treatment induces NV remodelling to have vascular loops, large core "feeder" vessels, anastomotic connections, and fewer branching capillaries (also known as abnormalization) [8, 26]. In this regard, the C + F + group is thought to be the result of abnormalization.

According to quantitative analysis, the C + F + group presents a larger NV area and longer total NV length as compared with the other two groups. Meanwhile, the C + F − group presented a lower NV area, shorter NV total length, and higher NV density than the C + F + group, which is thought to be indicative of a more compact structure than in NV patterns with more branching capillaries. In the comparison of quantitative values of NV between exudative and nonexudative lesions in the C + F + group, NVs with exudation were larger and longer with higher junction and endpoint numbers. Specifically, the endpoint number representing sprouting vessels at peripheral lesions of NV was the only parameter to show a statistically significant association with activity in both univariate and multivariate analyses. This was also consistent with the qualitative analysis outcome that the presence of peripheral tiny branching capillaries was related with exudation. Previously, we also reported that the endpoint number density of NV in type 1 AMD may be associated with a frequent recurrence of exudation [15]. With these results, the number of open-ended vessels is considered to be a quantitative indicator of activity.

The three groups stratified according to NV pattern displayed no statistical difference in duration of previous treatment, although number of previous anti-VEGF treatments was greater in the C + F + group than in the C + F − group (post-hoc paired analysis: *p* = 0.01).

Xu et al. [7] reported that presence of capillary fringe in a treatment-naïve state was associated with NV doubling during long-term follow-up. We speculated that the C +

F + group, which has larger and longer NV with larger core vessel calibre, includes abnormalized NV cases due to highly active sprouting vessels and IVI treatment. To figure out whether the NV pattern is different from that at the beginning of disease or is changed by repeated IVI treatment, further studies are needed in treatment-naïve patients.

In 12 months follow up analysis, exudation recurrence was observed in about 85% of patients who did not show exudation at the time of OCTA analysis. In particular, patients in the C + F− group, who did not show any exudation at the time of analysis, also showed exudation recurrence in 12 eyes (of 15 eyes). Among three patterns, the C + F + group needed large numbers of anti-VEGF injections during the 12 months regardless of exudation presence at the time of analysis. In addition, regardless of the type of NV in OCTA, recurrence occurs about 5–6 months after the preceding IVI, therefore, it is still difficult to predict NV activity through morphological classification of NV. Close follow up is considered necessary even in eyes which are maintained without exudation recurrence.

There are several limitations to this study including its retrospective, cross-sectional design and small number of subjects—in particular including in the C − F + and C + F − groups. Poorly segmented or visualised images due to large PED, submacular haemorrhage, or NV larger than the measurement area were excluded (16/112; 14.3%) and could have created a selection bias in favour of NVs with a hyperintense OCTA signal. However, the exclusion ratio is relatively lower than in other studies that used OCTA images in NVAMD (20–32%) [22, 27, 28].

In conclusion, this study suggests that the presence of peripheral branching capillaries can be used as an indicator of activity in qualitative and quantitative features in NV having fine branching vascular structures with or without core vessels.

Summary

What was known before

- The presence of tiny branching vessels, peripheral arcades, loops and perilesional halo were proposed as exudative biomarkers in AMD.
- In previous study, NV patterns were classified according to vascular morphology, such as "sea fan," "medusa," or "dead tree," which is tends to be subjective.

What this study adds

- After categorisation of type 1 NV patterns in AMD according core vessel and fine branching vessels, NV

morphology with fine branching vessels were considered to have exudative activity compared to NV without fine branching.

- In patterns with fine branching vessel, quantitative analyses revealed a significant correlation between peripheral tiny branching capillaries and exudative activity.
- Peripheral arcades, inner branching capillaries, and loops were not related with exudative activity.

Compliance with ethical standards

Conflict of interest The authors declare no competing interests.

Publisher's note Springer Nature remains neutral with regard to jurisdictional claims in published maps and institutional affiliations.

References

1. Spaide RF. Rationale for combination therapies for choroidal neovascularization. Am J Ophthalmol. 2006;141:149–56.
2. Huang D, Jia Y, Rispoli M, Tan O, Lumbroso B. Optical coherence tomography angiography of time course of choroidal neovascularization in response to anti-angiogenic treatment. Retina. 2015;35:2260–4.
3. Patel R, Wang J, Campbell JP, Kiang L, Lauer A, Flaxel C, et al. Classification of Choroidal Neovascularization Using Projection-Resolved Optical Coherence Tomographic Angiography. Invest Ophthalmol Vis Sci. 2018;59:4285–91.
4. Carnevali A, Cicinelli MV, Capuano V, Corvi F, Mazzaferro A, Querques L, et al. Optical Coherence Tomography Angiography: a Useful Tool for Diagnosis of Treatment-Naïve Quiescent Choroidal Neovascularization. Am J Ophthalmol. 2016;169:189–98.
5. Lupidi M, Cerquaglia A, Chhablani J, Fiore T, Singh SR, Cardillo Piccolino F, et al. Optical coherence tomography angiography in age-related macular degeneration: the game changer. Eur J Ophthalmol. 2018;28:349–57.
6. Kuehlewein L, Bansal M, Lenis TL, Iafe NA, Sadda SR, Bonini Filho MA, et al. Optical Coherence Tomography Angiography of Type 1 Neovascularization in Age-Related Macular Degeneration. Am J Ophthalmol. 2015;160:739–48.
7. Xu D, Dávila JP, Rahimi M, Rebhun CB, Alibhai AY, Waheed NK, et al. Long-term Progression of Type 1 Neovascularization in Age-related Macular Degeneration Using Optical Coherence Tomography Angiography. Am J Ophthalmol. 2018; 187:10–20.
8. Miere A, Butori P, Cohen SY, Semoun O, Capuano V, Jung C, et al. Vascular remodeling of choroidal neovascularization after anti-vascular endothelial growth factor therapy visualized on optical coherence tomography angiography. Retina. 2019;39: 548–57.
9. von der Emde L, Thiele S, Pfau M, Nadal J, Meyer J, Möller PT, et al. Assessment of Exudative Activity of Choroidal Neovascularization in Age-Related Macular Degeneration by OCT Angiography. Ophthalmologica. 2020;243:120–8.
10. Coscas F, Lupidi M, Boulet JF, Sellam A, Cabral D, Serra R, et al. Optical coherence tomography angiography in exudative age-related macular degeneration: a predictive model for treatment decisions. Br J Ophthalmol. 2019;103:1342–6.
11. Al-Sheikh M, Iafe NA, Phasukkijwatana N, Sadda SR, Sarraf D. Biomarkers of neovascular activity in age-related macular degeneration using optical coherence tomography angiography. Retina. 2018;38:220–30.
12. Richard G, Monés J, Wolf S, Korobelnik JF, Guymer R, Goldstein M, et al. Scheduled versus Pro Re Nata Dosing in the VIEW Trials. Ophthalmology. 2015;122:2497–503.
13. Kim SW, Oh J, Kwon SS, Yoo J, Huh K. Comparison of choroidal thickness among patients with healthy eyes, early age-related maculopathy, neovascular age-related macular degeneration, central serous chorioretinopathy, and polypoidal choroidal vasculopathy. Retina. 2011;31:1904–11.
14. Margolis R, Spaide RF. A pilot study of enhanced depth imaging optical coherence tomography of the choroid in normal eyes. Am J Ophthalmol. 2009;147:811–5.
15. Choi M, Kim SW, Yun C, Oh J. OCT Angiography Features of Neovascularization as Predictive Factors for Frequent Recurrence in Age-Related Macular Degeneration. Am J Ophthalmol. 2020; 213:109–19.
16. Zhao Z, Yang F, Gong Y, Yu S, Liu H, Wang H, et al. The Comparison of Morphologic Characteristics of Type 1 and Type 2 Choroidal Neovascularization in Eyes with Neovascular Age-Related Macular Degeneration using Optical Coherence Tomography Angiography. Ophthalmologica. 2019;242:178–86.
17. An D, Balaratnasingam C, Heisler M, Francke A, Ju M, McAllister IL, et al. Quantitative comparisons between optical coherence tomography angiography and matched histology in the human eye. Exp Eye Res. 2018;170:13–19.
18. Ghasemi Falavarjani K, Al-Sheikh M, Darvizeh F, Sadun AA, Sadda SR. Retinal vessel calibre measurements by optical coherence tomography angiography. Br J Ophthalmol. 2017;101:989–92.
19. Coscas GJ, Lupidi M, Coscas F, Cagini C, Souied EH. Optical coherence tomography angiography versus traditional multimodal imaging in assessing the activity of exudative age-related macular degeneration: a New Diagnostic Challenge. Retina. 2015;35: 2219–28.
20. Roberts PK, Nesper PL, Gill MK, Fawzi AA. Semiautomated quantitative approach to characterize treatment response in neovascular age-related macular degeneration: a Real-World Study. Retina. 2017;37:1492–8.
21. Zudaire E, Gambardella L, Kurcz C, Vermeren S. A computational tool for quantitative analysis of vascular networks. PLoS ONE. 2011;6:e27385.
22. Takeuchi J, Kataoka K, Ito Y, Takayama K, Yasuma T, Kaneko H, et al. Optical Coherence Tomography Angiography to Quantify Choroidal Neovascularization in Response to Aflibercept. Ophthalmologica. 2018;240:90–98.
23. Sulzbacher F, Pollreisz A, Kaider A, Kickinger S, Sacu S, Schmidt-Erfurth U. Identification and clinical role of choroidal neovascularization characteristics based on optical coherence tomography angiography. Acta Ophthalmol. 2017;95:414–20.
24. Karacorlu M, Sayman Muslubas I, Arf S, Hocaoglu M, Ersoz MG. Membrane patterns in eyes with choroidal neovascularization on optical coherence tomography angiography. Eye (Lond). 2019;33: 1280–9.

25. Miere A, Semoun O, Cohen SY, El Ameen A, Srour M, Jung C, et al. Optical coherence tomography angiography features of subretinal fibrosis in age-related macular degeneration. Retina. 2015;35:2275–84.

26. Spaide RF. Optical Coherence Tomography Angiography Signs of Vascular Abnormalization With Antiangiogenic Therapy for Choroidal Neovascularization. Am J Ophthalmol. 2015;160:6–16.

27. Uchida A, Hu M, Babiuch A, Srivastava SK, Singh RP, Kaiser PK, et al. Optical coherence tomography angiography characteristics of choroidal neovascularization requiring varied dosing frequencies in treat-and-extend management: an analysis of the AVATAR study. PLoS ONE. 2019;14: e0218889.

28. Farecki ML, Gutfleisch M, Faatz H, Rothaus K, Heimes B, Spital G, et al. Characteristics of type 1 and 2 CNV in exudative AMD in OCT-Angiography. Graefes Arch Clin Exp Ophthalmol. 2017; 255:913–21.